



Hydrogen retention to impurities in tungsten: A multi-scale study

K. Heinola*, T. Ahlgren

Department of Physics, University of Helsinki, P.O. Box 64, 00560 Helsinki, Association EURATOM-TEKES, Finland

ARTICLE INFO

Article history:

Available online 17 January 2013

ABSTRACT

The concept of numerically solving the rate theory equations was used in determining hydrogen retention to carbon, oxygen and argon impurities in bulk tungsten. In the simulations, a hydrogen pulse with low energy and low fluence was subjected to tungsten with varying impurity concentrations. Retention and release of hydrogen atoms from impurities and intrinsic high-energy traps was monitored during and after the pulse. At 500 K the detrapping of hydrogen and diffusion to the W surface was found to take place in long timescales after the pulse shutdown.

© 2013 Elsevier B.V. All rights reserved.

1. Introduction

Tungsten (W) has been chosen to be used as the divertor plate material in the next step fusion device ITER [1,2]. In JET ITER-like Wall (ILW) experiment the divertor region consists of bulk W tiles and W coated carbon-fiber tiles [3]. Both of these W materials contain intrinsic unavoidable impurities such as carbon (C) and oxygen (O). Concentrations can be up to ~few at.% depending on the processing method. In addition, due to the manufacturing process the W coating includes small traces of argon (Ar) as an impurity (~1 at.%) [4]. Hydrogen (H) has high mobility in W [5], but easily congregates in spacious defects such as grain boundaries, dislocations, and voids. Point defects like mono-vacancies, self-interstitial atoms (SIAs) and other impurity atoms can also act as hydrogen trapping defects.

In this work, hydrogen retention to bulk W containing varying amounts of C, O and Ar impurities was studied computationally. The retention and detrapping was monitored during and after a low-fluence, low-energy hydrogen pulse. The method used solves numerically a set of rate theory equations (RE) describing all the dynamic events occurring in the bulk and on the sample surface. Equations were parametrised with first-principles calculations using electron density functional theory (DFT) and with binary collision approximation (BCA) calculations. The length and time scales in the present methodology can vary from Å to meters and from femtoseconds to minutes, and is therefore referred as multi-scale method. The limitation with the rate equations is that the monitored concentrations are presented one-dimensionally as a function of depth, whereas there is no limitation in the number of particles and the time step of the dynamic processes can be uncomparable low but still keeping the simulation time in minute-scale with low computational cost.

2. Computational method and simulation setup

The simulation method utilized in the present work, solves a set of REs describing chemical reactions in the material. The concentration C for each examined distinct entity – as a function of depth and time – is given by the following coupled partial differential equations [6–8]

$$\frac{\partial C_\alpha(x, t)}{\partial t} = D_\alpha \frac{\partial^2 C_\alpha(x, t)}{\partial x^2} + S_\alpha(x, t) \pm \sum_{\beta, \gamma=1}^N k_{\beta, \gamma}^2 D_\beta C_\beta(x, t) \pm \sum_{\delta=1}^N v_\delta e^{-\frac{E_{A, \delta}}{kT}} C_\delta(x, t), \quad (1)$$

where α , β , γ and δ stands for hydrogen, vacancy, SIA, impurities (here as C, O and Ar), and combinations of all of them. In total there are N distinct entities, which are monitored simultaneously. Full description of entities included in the present RE method have been published recently [9].

The first term on the right-hand side of Eq. (1) describes the diffusion of an entity (α) with a diffusion coefficient (D_α). The second term (S_α) is the source term, which includes the irradiation and the resulting induced defects. The third term comprises all exothermic reactions, such as trapping and defect clustering, described with a sink strength $k_{\beta, \gamma}^2$. The last term in Eq. (1) is endothermic, and in general describes the reverse process of the previous term. This term includes hydrogen detrapping from point defects, grain boundaries, dislocations and impurities, and dissociation of vacancy and SIA clusters. The v_δ is pre-exponential factor for detrapping or dissociation, which includes an attempt frequency and geometrical factors, and $E_{A, \delta}$ is the minimum activation energy the system has to pass as the complex δ breaks up. The choice of plus and minus sign in the last two terms depends on the examined reaction. Detailed description of each of the terms, their numerical values and their implementation as well as

* Corresponding author.

E-mail address: kheinola@aclab.helsinki.fi (K. Heinola).

benchmarking of the present RE code against experiments have been presented previously [9].

The parametrization of RE's is the key issue in setting up a simulation describing dynamic effects [9]. The first-principles DFT calculations were performed for determining the fundamental energetics of H in bulk W with and without impurities. The calculations were performed with the Vienna Ab-initio Simulation Package (VASP) [10–12]. The electronic groundstate of the studied system was calculated using the projector-augmented wave potentials as provided in VASP [13,14]. The parameters used in the DFT calculations have been published previously and they have been verified to reproduce accurately the W bulk, surface and intrinsic point defect properties as compared to experimental and other DFT results found in the literature [5,15–17]. A body-centered cubic supercell with 128 lattice sites was used for describing W with impurities. The impurities were considered to be located in a substitutional lattice site. The binding energy of H atom to impurity was calculated as

$$E_b = [E_i + E_H] - [E_{i-H} + E_0], \quad (2)$$

where E_{i-H} and E_i refer to the total energy of an impurity system with and without hydrogen atom, respectively. E_H is the total energy of a H atom on the solute site in the bulk and E_0 is the reference energy of bulk W. If the binding energy calculated with Eq. (2) is positive, the H-impurity system is stable. To obtain reliable binding energy results computationally, the H atom should not be located in the vicinity of the impurity after detrapping, i.e. not be located in the same simulation cell with the impurity. Eq. (2) takes into account this condition by providing a possibility to consider detrapped H by placing it to a solute site.

The trapping energy is defined as the binding energy summed with the migration energy (E_m) of the particle with the lowest migration barrier, i.e. $E_t = E_b + E_m$. H diffusion parameters in pure bulk W ($D_0 = 4.8 \times 10^{-8} \text{ m}^2/\text{s}$, $E_m = 0.26 \text{ eV}$) were taken from previous work [17]. For light mass particles such as hydrogen, the vibrational effects can play an important role and the zero-point energy (ZPE) has to be taken into account [5]. Therefore, the trapping energy has been calculated with $E_t = E_b + E_m + \Delta\text{ZPE}$, where ΔZPE is the difference in ZPE's for systems of hydrogen bound to impurity and hydrogen dissociated from it. The ΔZPE for the present work was estimated from the previous results of hydrogen trapped to W mono-vacancy ($\Delta\text{ZPE} \sim 0.11 \text{ eV}$) [17].

The total time used in the RE calculations was 60 s of which the first 20 s the W sample was subjected to 50 eV H pulse with a fluence of $7 \times 10^{14} \text{ cm}^{-2}$, while keeping the sample temperature (T) constant at 500 or 800 K for 60 s. The maximum depth was set to 0.5 μm . The H range profile used in RE was evaluated with BCA calculations using SRIM software [18]. Using a BCA code is not the most accurate way to determine the low energy H implantation profiles in W, but the fast diffusion of H in W anyway rapidly smears out the resulted H profile.

Extensive reviews on hydrogen trapping mechanisms in metals can be found in the literature [19–21]. Experimental work has shown that several trapping sites for H with unequal energies are either present in W naturally or initiated with implantations. In the present work, the energy of the incoming hydrogen particles was far too low for creating collisional damage in the sample due to the relatively high displacement energy of W (90 eV) [22]. Moreover, the H fluence was kept low and the pulse duration was only 20 s. Low energy and low flux strongly suggest that no implantation-induced defects, such as Frenkel pairs, are created during the pulse. This well-motivated assumption rules out the possibility of having implantation-induced dislocations and loops being created in the sample, which could act as an additional trapping site for hydrogen and therefore they were not included in the present calculations. In addition, if thermal defect formation is assumed

to have an exponential dependence $\exp(-E_f/kT)$, the high formation energy (E_f) of W mono-vacancies (experimental: 3.7 eV (Ref. [23]), DFT: 3.34 eV (Ref. [15])) results in negligible amounts of W mono-vacancies being formed in thermal equilibrium: number of W vacancies formed at 800 K is $\sim 7 \times 10^1 \text{ cm}^{-3}$. It is evident, that the number of thermodynamically formed mono-vacancies increases significantly with E_f . For example, for copper $E_f = 0.9 \text{ eV}$ results in $\sim 2 \times 10^{17} \text{ cm}^{-3}$ mono-vacancies at 800 K. Therefore, intrinsic W mono-vacancy concentrations were excluded from these calculations. It is worth to mention, that real W samples usually contain vacancy type defects exceeding the thermodynamic equilibrium due to processing and fabrication steps, but the amount of these defects were not evaluated in this work.

3. Results and discussion

The DFT results for the H binding energies to C, O and Ar impurities at substitutional lattice sites were 1.25, 1.19 and 0.43 eV, respectively. No impurities placed in interstitial lattice sites were examined in this study. The low Ar binding energy suggests that Ar can act as a retention site for H at or near room temperature, but will release H promptly at elevated temperatures. The relatively high binding energy of C implies a long term retention for H.

The main impurity, excluding molybdenum, in a bulk W sample is C with concentration of $\sim 10 \mu\text{g/g}$ (typical high purity 99.99% polycrystalline W by Plansee AG), corresponding to about $10^{25} \text{ C atoms/m}^3$. From this value a constant C concentration of $5 \times 10^{18} \text{ cm}^{-3}$ was chosen to be used in these calculations. O concentrations ($\sim 5 \mu\text{g/g}$, Plansee AG) were chosen as 2.5 and $5 \times 10^{18} \text{ cm}^{-3}$ and Ar 0.5, 5 and $50 \times 10^{18} \text{ cm}^{-3}$. As was mentioned above, implantation-induced defects were not considered to be created within the sample. An intrinsic high-energy trap concentration of $3 \times 10^{18} \text{ cm}^{-3}$ was assumed in the sample. High-energy traps may comprise of bulk or volume defects or interfacial defects. The concentration used in these simulations corresponds a typical grain mean radius of $\sim 10 \mu\text{m}$, which will give a lower level estimate for the intrinsic deep trap concentration. The detrapping energy from these high-energy traps (2.03 eV) was estimated from recent H on W surface DFT calculations [16].

In Table 1 are summarized the main results after the 60 s simulations with varying impurity concentrations at 500 K. Nearly 45% of the H implantation fluence is backscattered from the sample surface, the retained H depends on the impurity concentration and the rest of H was found ending up to sample surface. The minimum amount of total retained H was found to be $\sim 6\%$ of the total fluence. In all of the studied cases the effect of C is notable. The binding energy of H to C is the main retention source for H. Keeping the C impurity concentration constant, the total H retention increases slightly with increasing the O impurity concentration. However, the H retention to C decreases as part of the implanted H is trapped

Table 1

Calculated hydrogen retention in W with different C, O and Ar impurity concentrations. Hydrogen implantation fluence was $7 \times 10^{14} \text{ cm}^{-2}$ and pulse duration 20 s. Tabulated retention values are recorded after 1 min.

impurity conc. ($\times 10^{18} \text{ cm}^{-3}$)			hydrogen retention at 500 K ^a ($\times 10^{13} \text{ cm}^{-2}$)	
C	O	Ar	Impurity retention	Total ^b retention
5	–	–	C: 1.5	2.4 (6.1%)
5	2.5	–	C: 1.3, O: 0.4	2.5 (6.6%)
5	5	–	C: 1.2, O: 0.7	2.7 (7.0%)
5	–	0.5	C: 1.5, Ar: \sim none	2.4 (6.1%)
5	–	5	C: 1.5, Ar: \sim none	2.4 (6.1%)
5	–	50	C: 1.5, Ar: 10^{-6}	2.4 (6.1%)

^a 800 K: retention only to high-energy traps with $\sim 10^{12} \text{ H/cm}^2$.

^b Retention to impurities and high-energy traps.

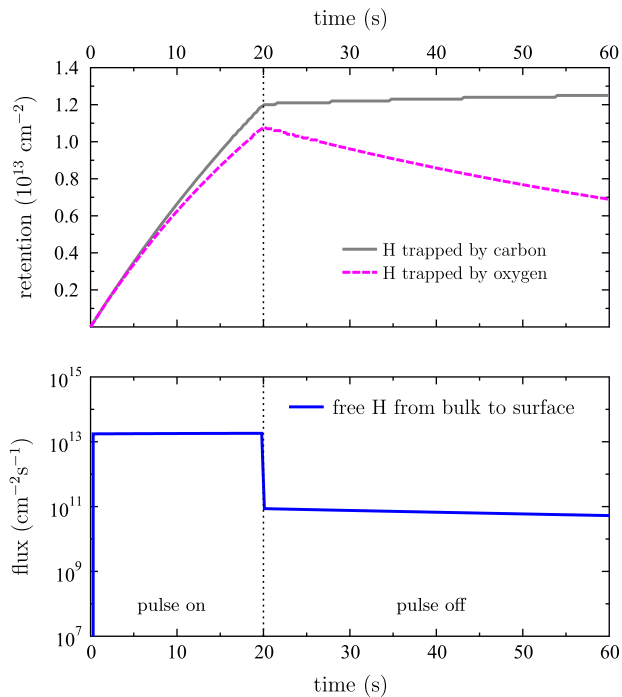


Fig. 1. Top: Exemplary RE calculation result for H retention in W at 500 K. The C and O impurity concentrations were $5 \times 10^{18} \text{ cm}^{-3}$ each. After the pulse, detrapping of H from O increases the retention to C. Bottom: Resulted flux of mobile H from the bulk to the surface. Flux is not terminated rapidly after the pulse due to the inventory of mobile H in the bulk.

by O. H trapping to Ar was found to be more or less negligible with all of the calculated concentrations. This is a clear demonstration that the low E_b of H to Ar is insufficient to retain H even at 500 K. Intrinsic high-energy traps were found to trap hydrogen $\sim 10^{13} \text{ cm}^{-2}$.

It is important to note that the retention and detrapping processes are dynamic effects in which the rates for retention and detrapping vary during the hydrogen pulse and the subsequent annealing. This effect can be clearly seen in Fig. 1, where H retention to $5 \times 10^{18} \text{ cm}^{-3}$ of C and O impurities at 500 K is presented as a function of time. Since the beginning of the H pulse, both C and O trap and detrap H atoms with unequal rates. Due to the difference in C and O E_b values, H is more easily detrapped from O, which is seen as a lower retention rate value from the beginning of the H pulse.

After the 20 s pulse, the O traps are slowly emptied from H which in turn increases the free mobile H concentration in the bulk. The free H ends up to the sample surface, diffuses deeper into the bulk or gets trapped with C. This can be seen as an increase in the C retained H concentration. Moreover, the H concentration diffusing to the surface does not decrease rapidly after the pulse. During the pulse, the flux of free H from the bulk to surface is $\lesssim 2 \times 10^{13} \text{ cm}^{-2} \text{ s}^{-1}$. After the pulse the flux decreases instantaneously to $\sim 1 \times 10^{11} \text{ cm}^{-2} \text{ s}^{-1}$ and in the end of calculation at 60 s the flux to surface is still $\sim 5 \times 10^{10} \text{ cm}^{-2} \text{ s}^{-1}$. Although the implantation fluence used in the calculated H pulse is fairly low, the results at 500 K obtained show clearly that the impurities, especially C, hinder the H out-diffusion from the sample. In Fig. 2 are presented the resulting concentration profiles of H trapped to C, O and high-energy defects in the end of the 60 s RE calculation at 500 K. In the course of implantation, the majority of the free H diffuses rapidly from the implantation zone ending up to the sample surface. This can be seen also in the shape of the trapped H profiles, where the retention maximum is near the surface. However, free H diffuses also deeper into the bulk where it gets trapped. The retention

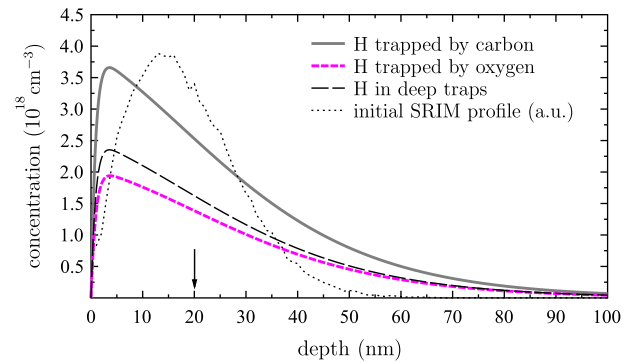


Fig. 2. Resulted concentration profiles of H trapped to C, O and high-energy traps in the end of 60 s RE run. C and O concentrations are same as in Fig. 1. Dotted profile is the SRIM calculated H profile used as implantation input in RE. Arrow represents the resulted approximative location of the interstitial H concentration profile maximum ($\sim 5 \times 10^{10} \text{ cm}^{-3}$) obtained with RE calculation.

profiles have tails with H concentration of $\sim 10^{10} \text{ cm}^{-3}$ as deep as 600 nm. It can be speculated, that with higher implantation fluences the H retention profile would extend deeper in the sample with higher concentration. At 800 K the H retention to C, O and Ar impurities is \sim null in the end of 60 s RE calculation run. The only trapping site for H are high-energy traps, where the retention concentration was found to be $\sim 10^{12} \text{ cm}^{-2}$, which is a factor of ten less than at 500 K.

To summarize, hydrogen retention was studied during and after a 50 eV/H pulse computationally with multi-scale RE calculations. Results show that C acts as an effective trapping site for H at 500 K whereas H was found to be trapped only to intrinsic high-energy traps at 800 K. At lower temperature also O impurity has an impact to the H retention, whereas the effect of Ar was found to be negligible. After the pulse the H flux from bulk to surface did not effectively drop to zero at 500 K, but instead was found to be slowly decreasing in the end of the monitoring time 60 s. This implies strongly that H will be released from W up to several minutes after the pulse, especially if the sample temperature gets lowered after the pulse. This prolonged out-diffusion is due to the H reserves at C impurities and high-energy traps which slowly release H at lower temperatures. The present C concentration corresponds to ~ 1 at.%, which is less than the reported values for C and O in the JET ILW W coatings 6 at.% [4]. Additional RE calculations will be performed with the representative ILW plasma and W coating impurity values.

Acknowledgments

This work, supported by the European Communities under the contract of Association between Euratom-Tekeles, was carried out within the framework of the European Fusion Development Agreement (EFDA). The views and opinions expressed herein do not necessarily reflect those of the European Commission. Grants of computer time from the Center for Scientific Computing (CSC) in Espoo, Finland are gratefully acknowledged.

References

- [1] ITER Physics Basis Editors, ITER Physics Expert Group Chairs and Co-Chairs and ITER Joint Central Team and Physics Integration Unit, Nucl. Fusion. 39 (1999) 2137.
- [2] A. Loarte, B. Lipschultz, A. Kukushkin, G. Matthews, P. Stangeby, N. Asakura, G. Counsell, G. Federici, A. Kallenbach, K. Krieger, et al., Nucl. Fusion 47 (2007) S203.
- [3] G.F. Matthews, P. Edwards, T. Hirai, M. Kear, A. Lioure, P. Lomas, A. Loving, C. Lungu, H. Maier, P. Mertens, et al., Phys. Scripta T128 (2007) 137.

- [4] C. Ruset, E. Grigore, I. Munteanu, H. Maier, H. Greuner, C. Hopf, V. Phylipps, G. Matthews, *Fusion Eng. Des.* 84 (2009) 1662.
- [5] K. Heinola, T. Ahlgren, *J. Appl. Phys.* 107 (2010) 113531.
- [6] A. McNabb, P.K. Foster, *Trans. Metal. Soc. AIME* 227 (1963) 618.
- [7] M.I. Baskes, W.D. Wilson, *Phys. Rev. B* 27 (1983) 2210.
- [8] S.M. Myers, P. Nordlander, F. Besenbacher, J.K. Nørskov, *Phil. Mag. A* 48 (1983) 397.
- [9] T. Ahlgren, K. Heinola, K. Vörtler, J. Keinonen, *J. Nucl. Mater.* 427 (2012) 152.
- [10] G. Kresse, J. Hafner, *Phys. Rev. B* 47 (1993) 558.
- [11] G. Kresse, J. Hafner, *Phys. Rev. B* 49 (1994) 14251.
- [12] G. Kresse, J. Furthmüller, *Phys. Rev. B* 54 (1996) 11169.
- [13] P.E. Blöchl, *Phys. Rev. B* 50 (1994) 17953.
- [14] G. Kresse, D. Joubert, *Phys. Rev. B* 59 (1999) 1758.
- [15] T. Ahlgren, K. Heinola, N. Juslin, A. Kuronen, *J. Appl. Phys.* 107 (2010) 033516.
- [16] K. Heinola, T. Ahlgren, *Phys. Rev. B* 81 (2010) 073409.
- [17] K. Heinola, T. Ahlgren, K. Nordlund, J. Keinonen, *Phys. Rev. B* 82 (2010) 094102.
- [18] J.B.J.F. Ziegler, M. Ziegler, *SRIM The Stopping and Range of Ions in Matter*, 2008 <<http://www.srim.org/>>.
- [19] C.A. Wert, *Hydrogen in Metals II*, Springer-Verlag, Berlin-Heidelberg-New York, 1978.
- [20] S. Picraux, *Nucl. Instr. Meth.* 182–183 (1981) 413.
- [21] S.M. Myers, M.I. Baskes, H.K. Birnbaum, J.W. Corbett, G.G. DeLeo, S.K. Estreicher, E.E. Haller, P. Jena, N.M. Johnson, R. Kirchheim, et al., *Rev. Mod. Phys.* 64 (1992) 559.
- [22] ASTM E521 –96(2009), *Standard Practise for Neutron Radiation Damage Simulation by Charged-Particle Irradiation*, vol. 12.02 (American Society for Testing and Materials, Philadelphia, PA, 2009).
- [23] K.-D. Rasch, R.W. Siegel, H. Schultz, *Phil. Mag. A* 41 (1980) 91.